Digest Journal of Nanomaterials and Biostructures Vol. 17, No. 3, July - September 2022, p. 759 - 770

The structural and figure of merit photodetector of PVP-doped with lanthanum

R. A. Ahmed[a,*], N. K. Hassan[b], I. M. Ibrahim[c]
[a]*Directorate of Education Salahuddin, Education Department of Tuz, Salahuddin, Iraq.*
[b]*Department of physics, College of Education for pure science, Tikrit university*
[c]*Department of physics, College of science, University of Baghdad, Baghdad, Iraq*

This study describes the fabrication and characterization of PVP and PVP/La thin films from a mixture of high molecular weight polyvinylpyrrolidone (PVP) and (1, 2, and 3)% lanthanum chloride using an electrospinning process on glass and silicon. It includes an N-type (Si) (111) substrate at room temperature. Field Emission Scanning Electron Microscopy (FESEM) analysis reveals fibers with an average diameter in the range of 125-250 nm. The mean fiber diameter decreases with increasing concentration (La). The optical energy gap was determined from the analysis of the transmission spectrum in the UV-visible region. The optical gap (E_g) gradually decreases from 4 eV to 3.64 eV for undoped PVP films due to the increase in La ion content at 3%, which determines the feasibility of using these obtained fibers in the manufacturing process. PVP/La nanofibers as detectors.

(Received February 21, 2022; Accepted July 10, 2022)

Keywords: Electrospinning, Thin film, PVP polymer, FESEM, Photoconductivity

1. Introduction

Polymers are one of the most frequently utilized materials in nanotechnology, particularly in the fields of nanofibers and nanocomposites. Hundreds of polymers, including natural and synthetic polymers, have been produced from nanofibers and nanocomposites over the past 20 years [1] due to their unique and controllable properties such as low cost, ease of manufacture, low density, insulation, and chemical inertness. In the last few decades, the amount and use of polymeric materials has grown a lot, and polymeric materials are increasingly replacing ceramic and metal products [2].The dissolution of the polymer mainly depends on the properties of the solute and the solvent, and the viscosity of the medium, the structure of the polymer, and the molecular weight of the polymer also have a certain influence. Dissolving the polymer is a two-step process that must be done slowly. The solvent molecules first diffuse into the polymer and form a swelling gel, and then the gel gradually breaks down to create the actual solution. This process can take several hours or more for high molecular weight polymers, depending on sample size, temperature, and other factors [1].

Fibers are a type of material that consists of continuous filaments or individually elongated lengths of material. High molecular weight induces an increase in viscosity for a given polymer concentration within a homogenous sequence of linear polymers. The polymer must have a molecular weight of at least 12,000 g/mol and the ability to crystallize in order to produce fibers [1,2]. For fiber production, close-packed linear and symmetrical polymers with no pendant groups are desirable. The process of forming fibers from a bulk polymer material is called spinning. The properties of a fiber depend not only on the polymer from which it is made, but also on the manufacturing process. There are several methods to produce nanofibers, one of which is electrospinning [2]. In this technique, a polymer solution consists of a predetermined mixture of polymers suspended in a solvent. Gravity creates a drop of polymer solution at the tip of the capillary and holds it in place by surface tension. Fiber formation begins when the electrostatic

---

[*] Corresponding author: aliahmedraoof@gmail.com
https://doi.org/10.15251/DJNB.2022.173.759

force exceeds the surface tension of the droplet. When the ejected jet stream narrows by colliding with itself owing to a rise in surface charge density due to solvent evaporation, the fiber is created [1,2]. Because of their increased surface area to volume ratio, nanofibers It greatly improves existing technologies and creates applications in new areas. Reinforcement fibers in composites, protective gear, filtration, medical devices, and electrical and optical devices are potential applications for nanofibers, and due to their large surface area, nanofibers can be used in electronic devices such as sensors and actuators to reduce reaction times to stimuli [2].

Due to their strong interaction with light, rare earth elements have intriguing optical properties [3,4]. They offer important advantages for semiconductors that are crucial for photoluminescence and other optical properties, and they can generate radiation with blue, green, and red light wavelengths. This includes all wavelengths for device function [4].

2. Experimental

2.1. Materials

Spinnable Fibers for the electrospinning solutions were made using high molecular weight polyvinylpyrrolidone (PVP), $(C_6H_9NO_n)_n$ with a K value of 90, (manufactured by Sigma Aldrich, USA, high purity (99.99 %), and lanthanum chloride, $(La\ Cl_3.7H_2O)$ with molecular weight 371.37 g/mol as the source of (La) ions.

2.2. Synthesis of pure PVP, PVP/La solution, and samples

To create spinning solutions, a polyvinylpyrrolidone (PVP) polymer was dissolved in ethanol. (1) g of PVP polymer was added to about (11.4) mL of 10% (wt) ethanol solution. For 6 hours, the solution was mixed at room temperature using a magnetic stirrer.The salt $(LaCl_3.7H_2O)$ was dissolved in ethanol solvent at room temperature for 2 h using a magnetic stirrer, then each concentration (1, 2, and 3 mL) was added individually to (9, 8, and 7 mL) of pure PVP solution and left for 3 h at room temperature on a magnetic stirrer, to obtain homogeneous solutions. This 10 ml solution was then put into three plastic syringes that had metal needles inside. One syringe had a metal needle for each concentration.

2.3. Electrospinning process and set up

The principle of "electrostatic attraction" of charges is used in fiber manufacturing technology. In the fiber manufacturing process, electrostatic forces are used in the electrospinning process. This is in contrast to traditional fiber spinning procedures, which rely on mechanical forces to generate fibers (melt, dry, or wet spinning). Electrospinning uses a high-voltage source to create an electric field between a capillary tip and a grounded collection. The solution has its own surface tension inside the capillary, which can be charged from the outside by applying a high voltage power supply at the tip. An electric field changes the shape of a suspended droplet of polymer solution from hemispherical to conical (known as a Taylor cone) at the capillary tip [5]. The solution is ejected towards the grounded metallic collector when the strength of the electric field is greater than the surface tension of the polymer solution [6]. The diameter of the fibers is reduced when the solvent evaporates rapidly during the elongation process, and continuous fibers from micro to nanoscale are formed within The nonwoven mat collected on the grounded surface [7]. In this work, the voltage utilized was 20 kV and the stream rate was 0.3 mL/h. The collector used was a (4 × 6) cm aluminum grid separated 15 cm from the needle tip.

3. Results and discussion

3.1. FESEM images

A morphological characterization of nanofibers was performed using field emission scanning electron microscopy (FESEM) with an acceleration voltage of 10 kV. Fig. (1) illustrates a FESEM image of the collected fiber mats as well as an EDS plot and histograms of the fiber diameter distribution. According to the morphology analysis, the applied electrospinning parameters enabled the creation of smooth polymeric nanofibers and other composite nanofibers. The average diameter of PVP nanofibers was 231 nm. However, the majority of fiber polymer diameter values were between 50 nm and 800 nm as shown in Fig. (1b).

Energy dispersive X-ray analysis, or EDS analysis, is also known as energy dispersive X-ray microanalysis. It is an analytical technique used to determine the elemental composition or chemical characterization of a sample. It is based on an interaction between an X-ray source and a sample. Its characterization skills are largely due to the basic premise that each element has a unique atomic structure, resulting in a distinct collection of peaks in its X-ray emission spectrum. including carbon (C), nitrogen (N) and oxygen (O), see Fig. (1.c).

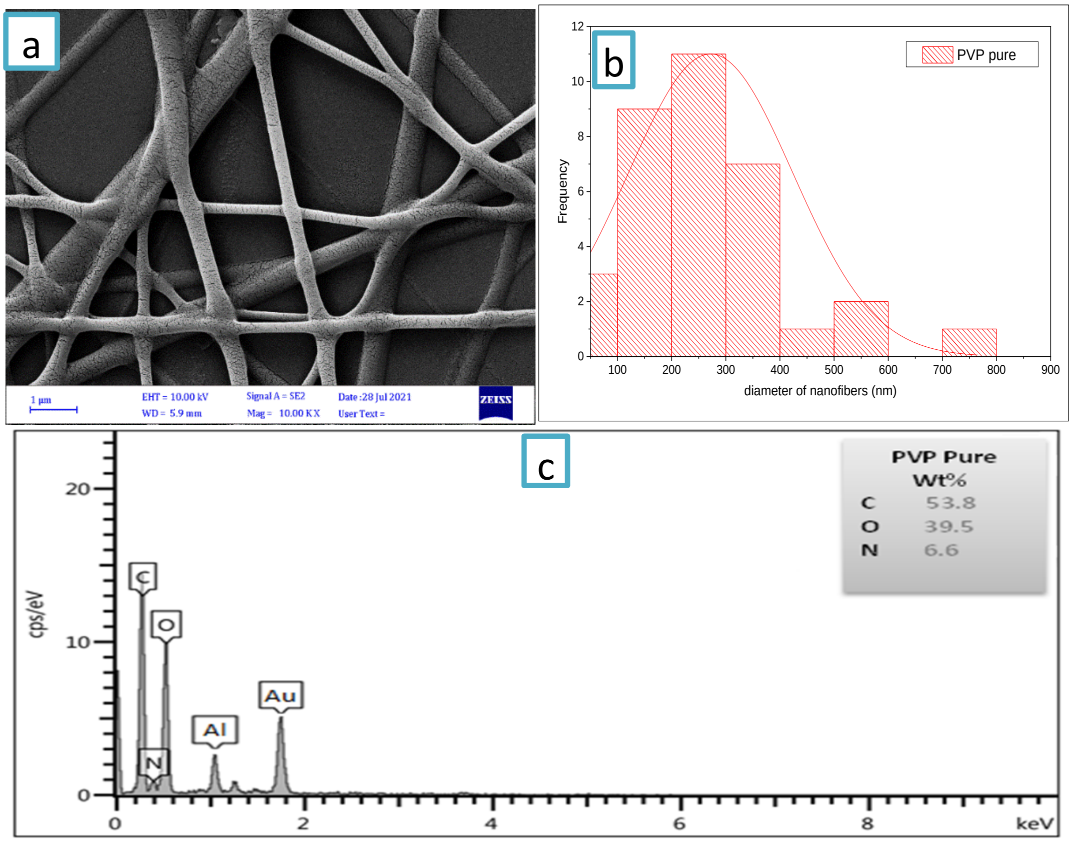

Fig. 1. a) FESEM images of PVP pure nanofibers with magnification of 10 K X. b) histograms of diameters with Gaussian distribution. c) EDS spectrum of PVP pure nanofibers.

Figures 1, 2, and 3 show FE-SEM images of the obtained fiber mats, as well as histograms of fiber diameter distribution and an EDX plot for PVP films doped with (La) in ratios of 1, 2, and 3%.According to the morphological study, the electrospinning settings used allowed the generation of very clear thin layers, which diffused well in alcohol without aggregation, and the additive salts were uniformly homogeneous in the polymer matrix. It was also found that the fibers were completely free of structural flaws. As shown in Table 1, the average value of the diameters of the PVP nanofibers decreased as the mass ratio of (La) increased. Based on the diameter distribution histograms, the statistical results showed that the average diameters of nanofibers for films are a few hundred and most values of the polymer fiber width range from 50 nm to less than 700 nm as the doping ratio increases. The presence of lanthanum at levels of 2% and 3% in dopes resulted in nanofibers with significantly smaller diameter values compared to the diameters of pure polymer nanofibers. This is due to the incorporation of an appropriate ratio of (La), which altered the movement and lengthened the spinning solution jet [6].

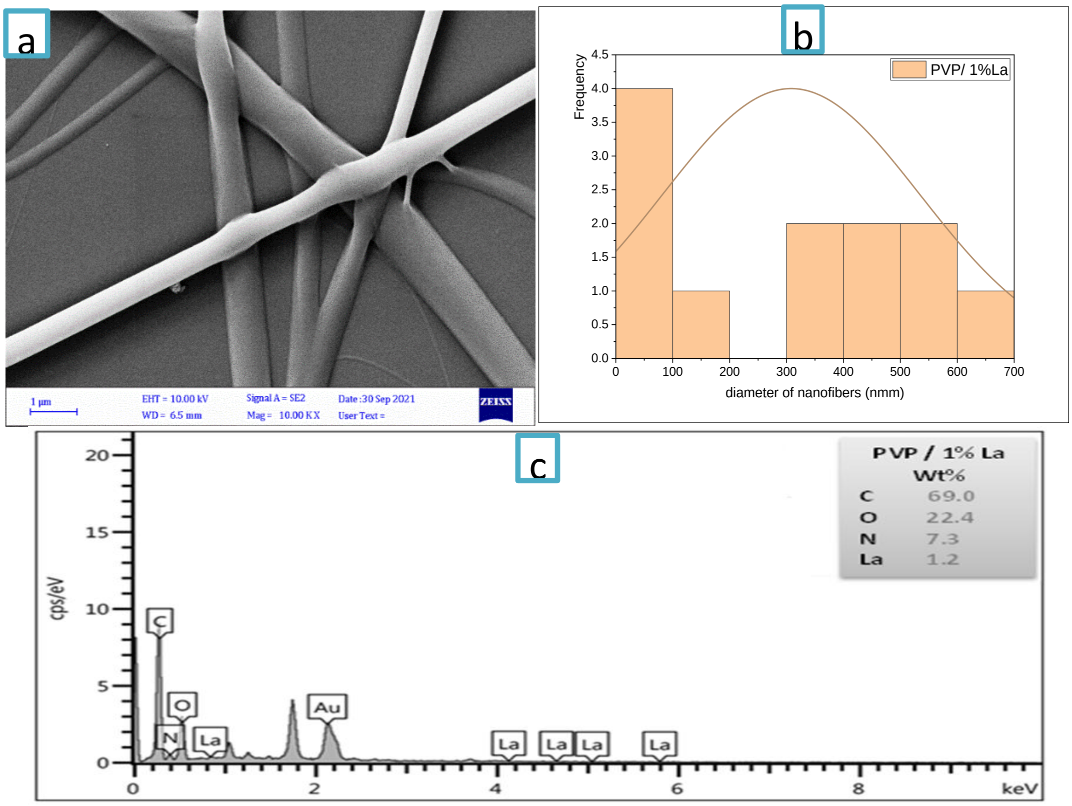

Fig. 2. (a) FESEM images of PVP/1%La nanofibers with magnification of 10 KX. b) histograms of diameters with Gaussian distribution. c) EDS spectrum of PVP/1%La nanofibers.

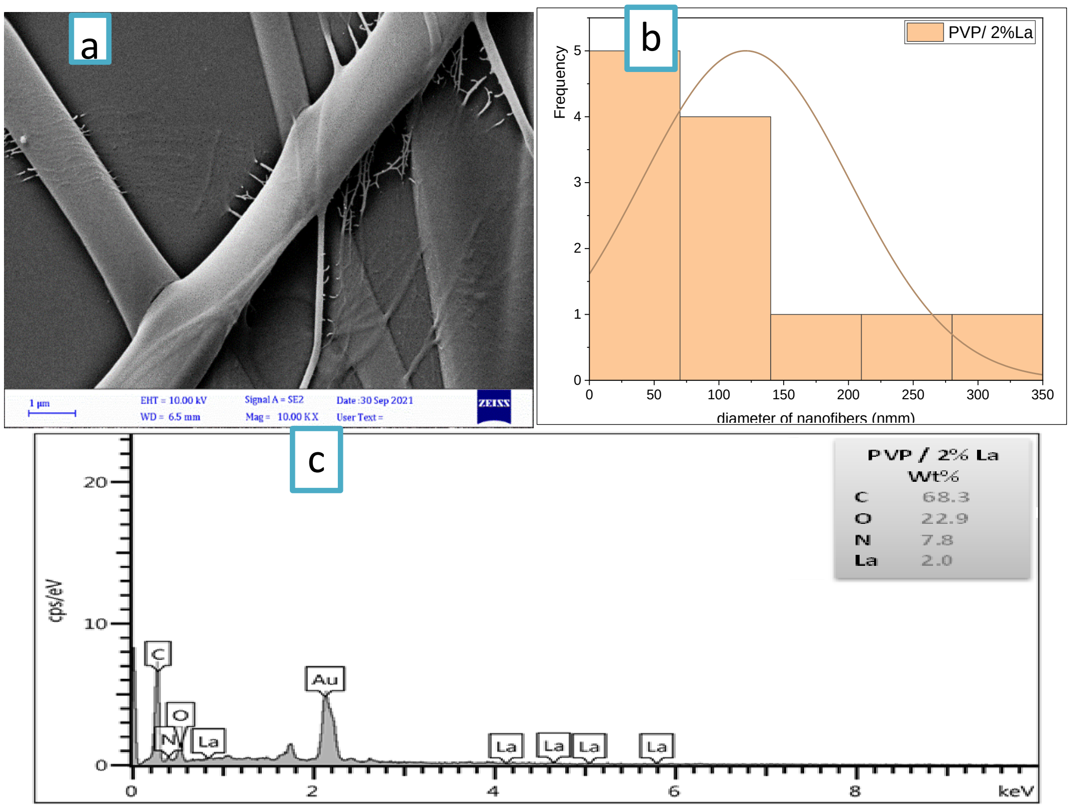

Fig. 3. a) FESEM images of PVP/2%La nanofibers with magnification of 10 KX. b) histograms of diameters with Gaussian distribution. c) EDS spectrum of PVP/2%La nanofibers.

Because of an increase in conductivity during high voltage application, the diameter of composite nanofibers is noticeably different from a pure polymer solution [7, 8]. Furthermore, a dependency between the decrease in diameter values of PVP/La nanofibers and the increase in specific surface area of composite fiber mats is observed, presenting a tremendous opportunity for organic and inorganic ultra-sensitive gas sensor applications [9]. The results of the EDS analysis for PVP/La samples are shown in Figures (2c, 3c, and 4c) and Table (2), with a slight difference between the material charge ratio and the actual element content in the samples attributed to the presence of an error rate in the measurement accuracy of the equipment used to calculate the weight of the doped material. It can be shown that C is the dominant element in the samples and the La content increased with an added amount of lanthanum, which was recognized as 1%, 2%, and 3%, respectively. The EDX spectrum of composite fiber mats shows five expected peaks corresponding to carbon (C), oxygen (O), nitrogen attributed to the chemical formula of the polymer, lanthanum (La) from the doping phase and gold (Au) peak in the sprayed gold layer for better conductivity in the FE-SEM examination.

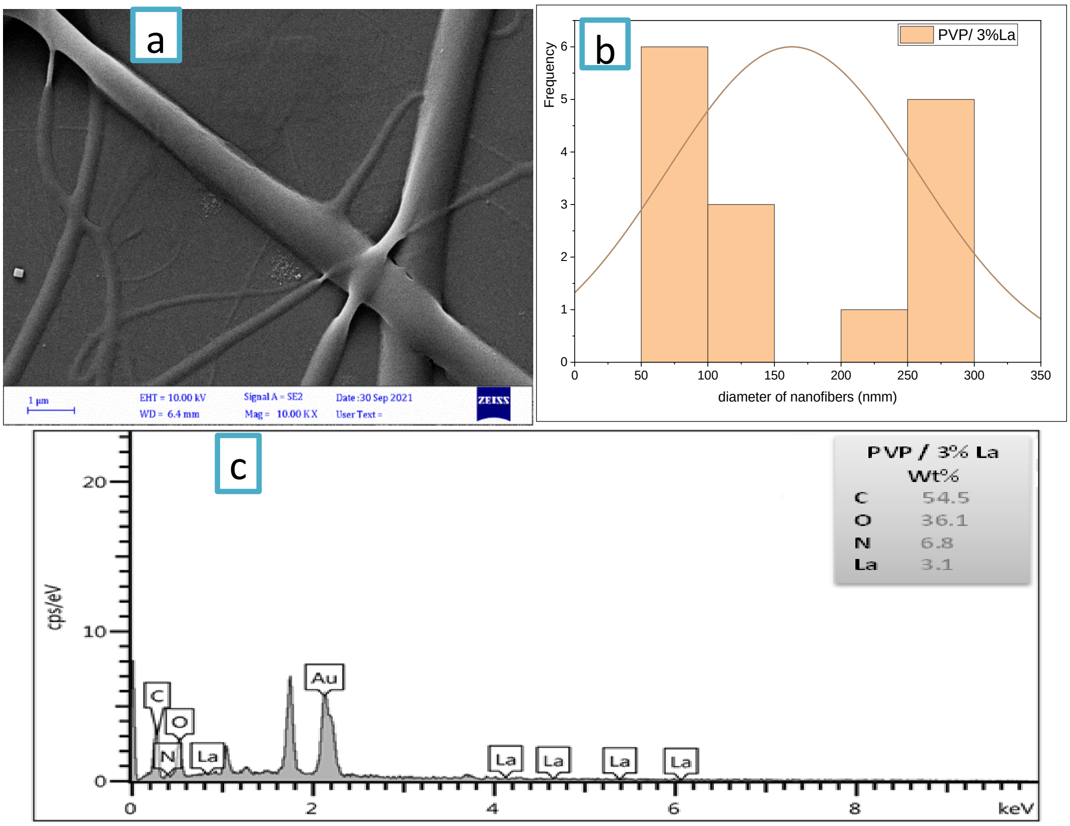

Fig. 4. a) FESEM images of PVP/3%La nanofibers with magnification of 10 KX. b) histograms of diameters with Gaussian distribution. c) EDS spectrum of PVP/3%La nanofibers.

Table 1. Average diameter of nanofibers for PVP/La films doped at different ratios.

Sample	PVP pure	PVP/1%La	PVP/2%La	PVP/3%La
Average diameter(nm)	231	250	125	169

Table 2. Shows the proportions of the elements present of PVP/La films doped at different ratios.

Sample	PVP pure	PVP/1%La	PVP/2%La	PVP/3%La
Carbon (C) %	53.8	69	68.3	54.5
Oxygen (O) %	39.6	22.4	22.9	36.1
Nitrogen (N) %	6.6	7.3	7.8	6.8
Lanthanum (La)%		1.2	2	3.1

3.2. Analysis of optical properties

The absorption coefficient (υ) at the frequency associated with the high absorption region can be determined directly from the absorption (A) and the film thickness () using the relationship [10].

$$a = 2.303\ A/\ t \tag{1}$$

where A is the absorbance and t is the thickness of the film. The fundamental absorption edge is one of the most important features of the absorption spectra of crystalline and amorphous materials. The basic absorption corresponds to the transition from the valence to the conduction band, from which the band gap of the material can be determined. The energy band gap () was estimated using [11].

$$\alpha h\upsilon = \beta(h\upsilon - E_g)^r \tag{2}$$

where β is a constant that depends on the probabilities of electron transitions, E_g is the optical energy gap, and r equals 0.5, which corresponds to each allowed direct optical transition.

Fig. (5) shows the absorption spectra of organic polymer PVP and PVP doped with three different concentrations of (La) (1, 2 and 3)%. It can be observed that the absorption is high, which means the absorption coefficient is greater than (10^4 cm^{-1}). Hence, it would be better to conclude that the grown nanostructures show good absorption in the UV-visible region of the electromagnetic spectrum. In both spectra, films have two peaks: B-band at wavelengths between (330-360) nm and Q-band at wavelengths between (360-700) nm. The absorption spectrum of the polymer gradually increases with the addition of lanthanum. This indicates that lanthanum is incorporated into the PVP matrix without changing the chemical structure of the polymer. With increasing (La) concentration seen in Fig. 5, the absorption spectra indicates a minor shift toward longer wavelengths, which is consistent with study [12]. With the increase of the doped phase in the form of (La), the absorptivity increases compared to pure polymer nanofibers. However, in the case of PVP/La composite nanofibers, an additional edge with a wavelength of 420 nm can be observed, which is due to the presence of (La) particles [13]. Fig. (5) shows the broadening of the UV-Vis spectrum in comparison between different concentrations of (La) the doped organic polymer. It is likely that slight molecular orbital hybridization is achieved between the HOMO of PVP and the LUMO of (La) [14]. The extension of the absorption level into the near-ultraviolet region in composite nanofibers doped at 1% to 3% concentration can be explained by a sufficient lanthanum concentration for the polymer, indicating that the polymer matrix plays a major role in the mechanism of electromagnetic radiation absorption for wavelengths below 350 nm. The noticeable increase in absorbance and the broadening of the absorption spectra of electromagnetic radiation from 320 to 350 nm wavelength, caused by an increase in lanthanum mass concentration in the polymer matrix, opens a wide range of potential applications of this type of material, in particular in optical shields [15]. The Tauces equation, used to estimate the value of the optical energy gap with the type of optical transition by plotting the relationship of $(\alpha h\upsilon)^2$ versus the photon energy ($h\upsilon$), was used to calculate the value of the optical energy gap (E_g) to calculate PVP-pure and PVP-doped thin films. It is clear that pure PVP and PVP-doped thin films have a direct energy gap.

Fig. (6) shows the energy gap that decreases with increasing volume ratios of La, Table (3) shows the optical direct energy gaps of pure PVP and PVP-doped thin films, with the first Eg representing Q-band and the second E_g represents B-Band.

The energy gap for pure polymer PVP nanofibers was (4 eV), which agrees with the results obtained in the papers [16, 17]. From Fig. 6, it can be seen that these direct energy gap values started to decrease with doping from (1 to 3)% from (4 eV) for pure PVP to (3.64 eV) for PVP/ 3% La. The significant decrease in the determined values of the direct optical band gaps can be attributed to the strong influence of La $^{+3}$ ions in modifying the electronic structure of the PVP dielectric. The La^{+3} ions are responsible for creating localized trapping levels within the bandgap, accelerating the low-energy transition and causing the optical bandgap to change [18]. The La particles with a mass concentration of (1, 2 and 3)%, due to the significant amount of semiconductor-enhancing phase particles, taking into account the decrease in fiber diameter values during the electrospinning process and an additional increase in specific surface area, make such a nanocomposite material particularly attractive in a wide range of applications such as sensors.

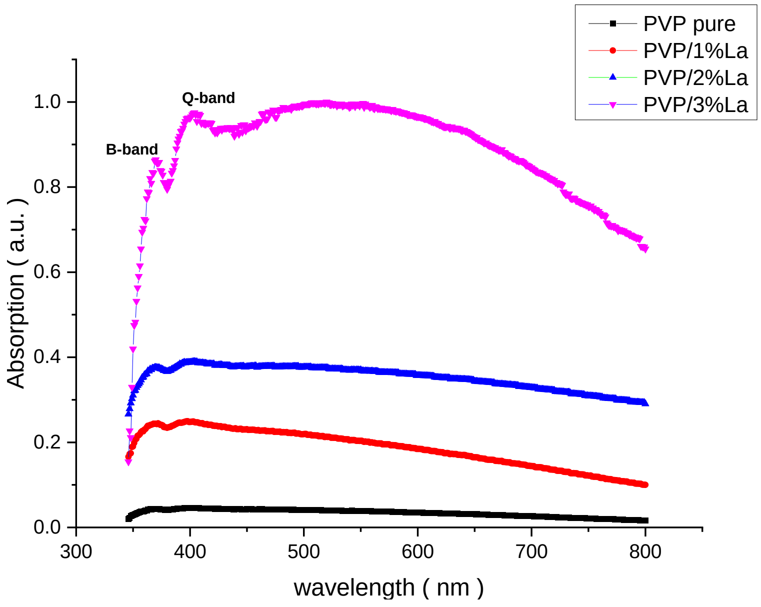

Fig. 5. The absorption spectra of pure PVP and PVP/La at doping ratio (1, 2, and 3)% thin films.

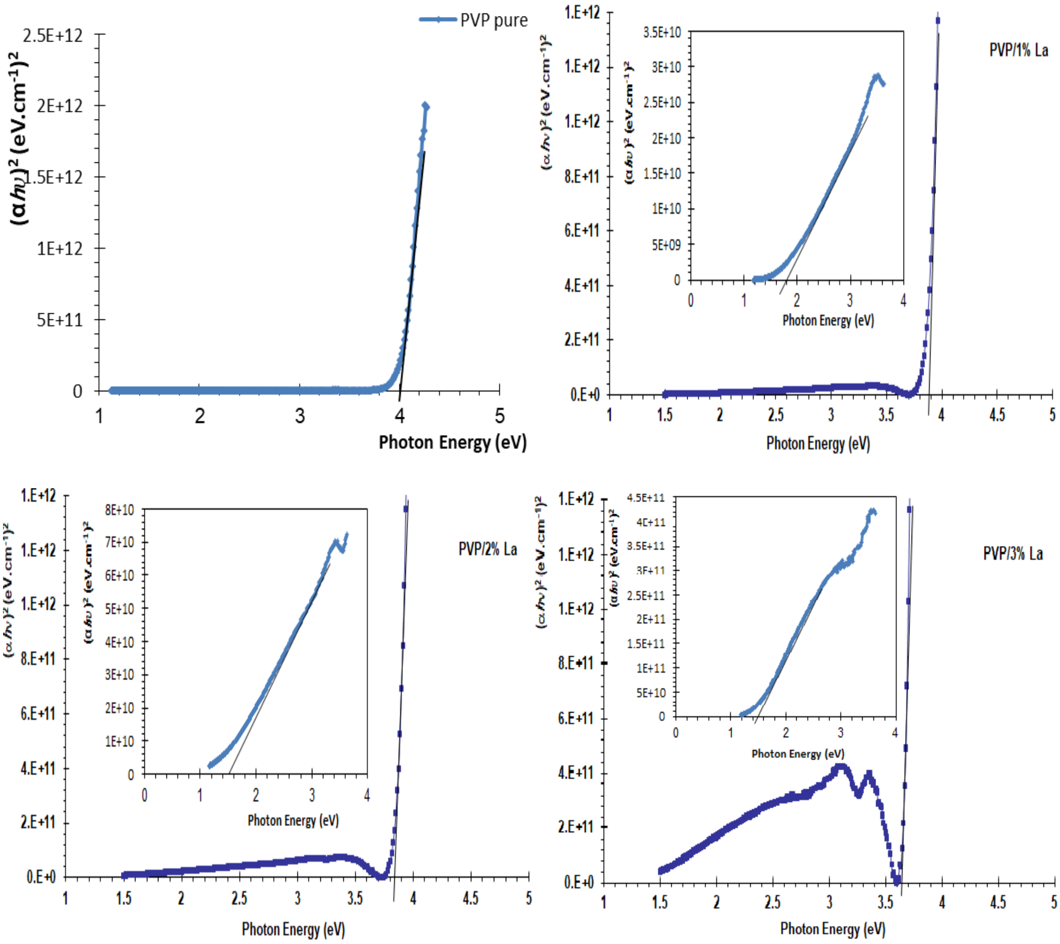

Fig. 6. $(\alpha h\upsilon)^2$ versus photon energy ($h\upsilon$)of incident radiation for pure PVP and PVP/La at doping ratio (1, 2, and 3)% thin films.

Table 3. Energy gaps of B-Band and Q-Band for PVP/La La at doping ratio (1, 2, and 3)% thin films.

sample	E_g of Q – Band (eV)	E_g of B – band (eV)
PVP pure	-	4
PVP/ 1%La	1.8	3.88
PVP/ 2%La	1.5	3.84
PVP/ 3%La	1.48	3.64

3.3 Photoconductivity

Photoconductivity (PC) is a useful tool for studying semiconductor materials such as the nature of photoexcitation and recombination processes. The conductivity of the material depends on the carrier lifetime, the carrier density, and the complex process of recombination, trapping, and carrier generation [19]. The trapping states or recombination centers in a forbidden energy zone of a photoconductor are known to affect the rise and fall curves of the photocurrent. The type and distribution of traps and recombination centers can thus be derived from these curves [20,21]. Photodetection occurs when a photodetector is repeatedly exposed to light with a specified wavelength (ON-OFF). The rise and fall times of a photodetector's response to a square-pulse signal are used to measure its speed in the time domain.

Rise time (τ_r): This is the time it takes for the detector output to switch between certain percentages (10% to 90%) of the peak value during rapid illumination [22]. Choosing a detector with a rise time of 1/10th the smallest pulse duration to be detected is a good working rule. This parameter is sometimes expressed in terms of detector bandwidth [23], where

$$\tau_r = \frac{0.35}{\Delta f} \tag{3}$$

Fall time (τ_f): When the light is off, the fall time (τ_f) is the time it takes for the detector to return to its initial pre-illuminated current value (i.e., dark state). In other words, it is the time it takes for the response to drop from 90% to 10% of its maximum value [22].

3.3.1. Time-Dependent Photocurrents

The time-dependent photocurrents of (La)-doped PVP polymer at different volume ratios (1, 2, and 3) % are shown in Figure (7). The most important properties of photodetectors are fast response (response) and fall times, from this figure the sensitivity values of pure and doped PVP thin films were calculated using the relationship [24]:

$$S = (I_{ph} - I_d)/ I_d \times 100\% \tag{4}$$

I_{ph} is light current and I_d is dark current

The sensitivity was measured at the excitation wavelengths λ_{exc}= (350) nm, where The light was turned ON and OFF every 20 seconds.

The best sensitivity value was 93.75% for the PVP/3% La photodetector as shown in Table (4). Fig. (7) shows that the current increases gradually with increasing volume ratios of (La). PVP and PVP/La composites absorb photons when their energy is equivalent to or higher than the frequency range of the semiconductor [25], resulting in the generation of electron-hole pairs in the semiconductor PVP/La. Simesquare pulses can be observed, indicating a fast response to light wavelength (see figure (7)) and, as shown in Table (4), a faster rise time for PVP/3% La film. This is probably due to the normal nanostructure of the sample as measured by the FESEM measurement, while the full-time increased with increasing doping ratio.

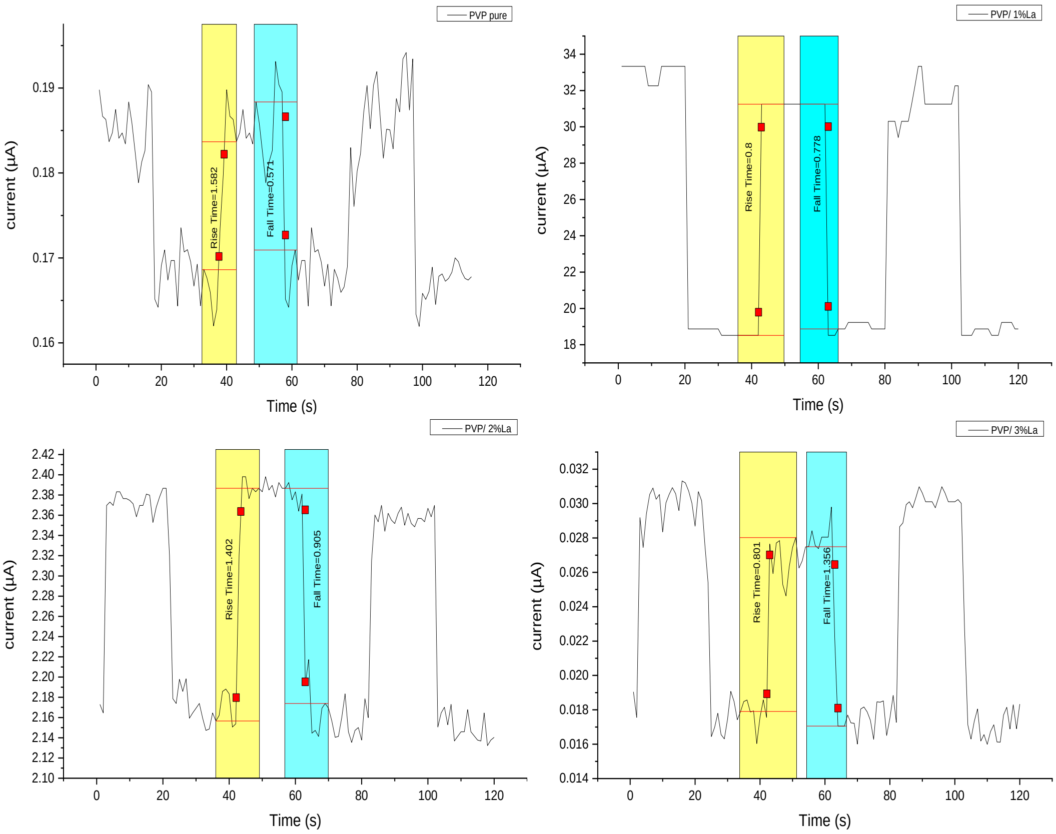

Fig. 7. The time-dependent photocurrent of the PVP and PVP/La concentrations (1, 2, and 3)% of La photodetector under λex. 350 nm.

Table 4. Rise time and Full time for pure and doped PVP polymer at different ratio of La.

parameter	**PVP pure**	**PVP/1%La**	**PVP/2%La**	**PVP/3%La**
S%	**19.753**	**76.657**	**12.265**	**93.750**
Rise time (s)	1.582	0.800	1.664	0.762
Fall time (s)	0.571	0.770	0.829	1.416

3.3.2. Responsivity

Spectral responsivity (R_λ) is a performance parameter, is defined as the photocurrent generated per unit power of incident light intensity on effective areas. The following relationship was used to calculate responsivity [23]:

$$R_\lambda = \frac{J_{ph}(\lambda)}{P_{in}(\lambda)} \tag{5}$$

where $P_{in}(\lambda)$ is the incident power density, and $J_{ph}(\lambda)$ is the photocurrent density from the tested detector. The responsivity is usually highest in the wavelength range where the photon energy is slightly higher than the bandgap energy, and decreases rapidly in the bandgap range where absorption decreases [26].

The responsivity is a study of pure PVP and PVP mixture with (La) films as a composite detector deposit on a Si-N type (111) substrate at the excitation wavelengths λ_{exc} = 350 nm and an intensity of 5 x 10 $^{-4}$ W/cm2. The responsivity for all samples increases with increasing volume ratio of (La) at (1, 2 and 3)% compared to pure PVP film which are higher responsivity values at 1% ratio of (La) (0.434 A/W) as shown in Table (5).

3.3.3. Quantum Efficiency (QE) or (η)

The following equations can be used to represent the QE. [23]:

$$\eta = \frac{N_e}{N_{ph}} \tag{6}$$

where $N_{ph}$is the incident or absorbed photon rate, $\mathbf{N_e}$ is the rate of photoelectron generation. The relation between responsivity R(λ) and η(λ) can be shown using the following expression [23]:

$$\eta(\lambda)=1240/(\lambda(nm))\times R(\lambda)\times 100\% \tag{7}$$

Table (5) shows that the quantum efficiency (η) value for pure PVP film is (0.098%), while the values for all films increase with increasing volume ratios of (La) compared to pure PVP film, with the higher value (154.07%) for the 1% ratio of (La).

3.3.4 The Noise-Equivalent Power (NEP) is expressed as [24]:

$$NEP = \frac{I_n}{R_\lambda} \quad \text{Watts} \tag{8}$$

where I_n is noise current (with dark current noise dominant), and noise current is defined by [32]:

$$I_n = \sqrt{4K_BT * \frac{\Delta f}{R_d}} \tag{9}$$

where Δf is the bandwidth, R_d is the detector's resistance in the dark. As the NEP decreases, the detection ability of the detector improves. Table 5 shows the equivalent noise power. In general, the (NEP) values of PVP/La decrease as the rate of (La) increases, the (NEP) value of pure PVP film is (9.03 × 10 $^{-11}$ W), while it is a lower value (0.0867 x $^{10-11}$ W), with the detection capability of the detector improving as the NEP decreases [24].

3.3.5. Detectivity (D) and Specific Detectivity (D^*)

An important figure of merit of a photodetector is its detection capability, which relates to the smallest significant optical signal that is distinguishable from noise. it is equal to the inverse of the noise power (NEP). It is denoted by D and measured in units (W^{-1}) [23]

$$D = \frac{1}{NEP} \tag{910}$$

The specific detectivity, or D* can be expressed as [23]:

$$D^* = \frac{\sqrt{\Delta f \cdot A_d}}{NED} \tag{11}$$

where A_d is active area of the detector.

As can be seen in Table (5), the highest values of detectivity and specific detectivity were at a doping ratio of 1% of (La), this may be due to a decrease in the NEP value of the film, and as a result, the detectability of the detector is improved.

Table 5. The detector parameters values of PVP and PVP with La mix at 350 nm.

parameter	PVP pure	PVP/1%La	PVP/2%La	PVP/3%La
R_λ (A/W)	0.00027	0.434	0.032	0.00041
η(%)	0.098	154.07	11.384	0.133
NEP (W)	$9.03x10^{-11}$	$0.0867x10^{-11}$	$0.302x10^{-11}$	$3.05x10^{-11}$
D (W^{-1})	$1.11x10^{10}$	$115x10^{10}$	$33.07x10^{10}$	$3.28x10^{10}$
D^* (cm. $Hz^{1/2}$ /W)	$0.201x10^{10}$	$29.4x10^{10}$	$6.37x10^{10}$	$0.835x10^{10}$

4. Conclusions

A typical electrospinning setup and high molecular weight PVP polymer were used to fabricate pure PVP and PVP/La composite nanofibers with smooth surfaces and uniform shapes. The fiber diameter varied from 125 nm to 250 nm. The optical measurements show the improvement in absorbance of PVP/La compared to pure PVP, and all samples have a direct energy gap and pick up (3%) with increasing (La) doping ratio (3.64 eV). The figure of merit of the photodetector explained that the addition of rare earth elements such as (La) improved the quantum efficiency (η) and the best doping ratio was 1%. It also led to an improvement in the sensitivity of the photodetector.

References

[1] Ramazan Asmatulu, Waseem S. Khan, Micro and Nano Technologies, 2019; https://doi.org/10.1016/B978-0-12-813914-1.00013-4

[2] Frank K. Ko, and Yuqin Wan, "Introduction to Nanofiber Materials", materials research society, 2014.

[3] K. Deshmukh, M. Mukherjee, S. Bhushan, R.C. Agrawal, Recent Research in Science and Technology, 4, 8 (2012) 55-57.

[4] D. Govindarajan and C. K. Nithya International Journal of Scientific & Engineering Research, 5, 12 (2014) 427-430. [6] M. Keikhaei, L. Motevalizadeh, E. A. Kakhki, International Journal of Nanoscience, 15, 3 (2016) 1-5.

[5] Taylor G. Electrically driven jets. Proc R Soc Lond A: Math Phys Eng Sci. 1969;313(515):453-475; https://doi.org/10.1098/rspa.1969.0205

[6] Taylor G., Proc R Soc Lond A: Math Phys Eng Sci. 1964;280(1382):383-397; https://doi.org/10.1098/rspa.1964.0151

[7] Doshi J, Reneker DH. Electrospinning process and applications of electrospun fibers. Conference Record of the 1993 IEEE Industry Applications Society Annual Meeting, 1993; IEEE; 1993. p. 1698-1703.

[8]. D. H. Reneker, and I. Chun, Nanotechnology, vol. 7(3), pp. 216-223, 1996; https://doi.org/10.1088/0957-4484/7/3/009

[9]. F. K. Ko, et al. "Structure and properties of carbon nanotube reinforced nanocomposites," in Proceedings of the 43rd Structures, Structural Dynamics and Materials Conference, vol. 3, pp. 1779-1787, Derver, Co, April 2002.

[10] Davis, E. A. & Mott, N. F., Phil. Mag. 22,903-922 (1970); https://doi.org/10.1080/14786437008221061

[11] M. Afzali, A. Mostafavi, and T. Shamspur, Materials Science and Engineering: C, (68), 789-797, 2016; https://doi.org/10.1016/j.msec.2016.07.038

[12 T. Gutul, E. Rusu, and N. Condur, Bellstein J. Nanotechnol., (5), 402-406, 2014; https://doi.org/10.3762/bjnano.5.47

[13] A.M. Abdelghany, E.M. Abdelrazek, S.I. Badr, Materials & Design, (57), 532-543, 2016; https://doi.org/10.1016/j.matdes.2016.02.082

[14] H. Méndez, G. Heimel, A. Opitz, K. Sauer, P. Barkowski, M. Oehzelt, J. Soeda, T. Okamoto, J. Takeya, J.-B. Arlin, J.-Y. Balandier, Y. Geerts, N. Koch, I. Salzmann, Angew. Chem. 125, 1, 7751-5 2013; https://doi.org/10.1002/anie.201302396

[15] R.S. Sabry, F.S. Mohammed, and R.A.A. Alkareem, "Fabrication of electro spinning 1D ZnO Nano fibers as UV-Photoconductor", Eng. & Tech.Journal, 2015;33.

[16] T. Tański and W. Matysiak, Journal of Achievements in Materials and Manufacturing Engineering, (82/1), 5-11, 2017; https://doi.org/10.5604/01.3001.0010.2071

[17] T. Tański, W. Matysiak, Ł. Krzemiński, et al., Applied Surface Science, (424), 184-189, 2017; https://doi.org/10.1016/j.apsusc.2017.02.258

[18]F.M. Ali, R.M. Kershi, M.A. Sayed, Y.M. AbouDeif Physica B:Physics of Condensed Matter (2018); https://doi.org/10.1016/j.physb.2018.03.031

[19] T. Tański, W. Matysiak, Ł. Krzemiński, et al., Applied Surface Science, (424), 184-189, 2017; https://doi.org/10.1016/j.apsusc.2017.02.258

[20] Callister J. and Malinowski S., "Optical Properties In Anderson", Materials Science and Engineering: An Introduction (6th). John Wiley & Sons, Inc.: New Jersey, 707-729, 2003.

[21] Joshi N.V., "Photoconductivity: Art, Science, and Technology", Marcel Dekker, New York, 1990.

[22] Srivastava S., Mishra S. K., Yadav R. S., Srivastava R. K., "Photoconductivity and Darkconductivity Studies of Mn-Doped ZnS Nanoparticles", J. Nanomaterials and Biostructures, 5, 1, 161 - 167, 2010.

[23] Shankar R., Srivastava R. K. and Prakash S. G., "Photoconductivity and Darkconductivity in ZnO: Cu, Br", J. Int. Academy of Physical Sciences, 16, 3, 283-288, 2012.

[24] Lui,J.M., "Photonic Devices", Cambridge University Press: Cambridge, ISNB 0521551951, 2005.

[25] Bahl I., Fundamentals of RF and Microwave Transistor Amplifiers, John Wiley and Sons, ISBN: 978-0-470-39166, p. 34, 2009; https://doi.org/10.1002/9780470462348

[26] Vandervalk C. J., Wenckebach T., and Planken P. C., J. Opt. Soc. Americ. B, 21, 3,622-631, 2004; https://doi.org/10.1364/JOSAB.21.000622